Quantifying Systematic Errors in Cluster Lens Models due to Cosmological Large-Scale Structures

RUTGERS
Aresty Research Center for Undergraduates

Aniruddha Madhava, Dr. Charles Keeton

Department of Physics and Astronomy, Rutgers University, Piscataway, New Jersey 08854

Introduction

- **Gravitational Lensing:** Deflections and distortions in light rays due to mass curving spacetime.
  - Lensing by galaxy clusters acts as **strong cosmic telescopes** that magnify the distant universe
  - Quantified by **deflection angles**
- **Cosmological Large-Scale Structures:** Largest structures in the universe, composed of matter that extend between galaxy clusters.
  - **Cosmic webs;** isotropic at cosmic scales (100 Mpc); filled with **voids** and **over-densities [1]**
- **Hubble Frontier Fields (HFF):** Commitment by the Hubble Space Telescope and the Space Telescope Science Institute to explore the early universe through observations of galaxy clusters. **[2]**

Motivation

Why?

1. **How did galaxies form?**
2. **How do primordial galaxies differ from "younger" galaxies?**
3. **What was star formation like in the early universe?**

Cluster lenses act as strong cosmic telescopes, revealing the distant, early universe [3,4,5]. If we want to use cluster lensing to peer back, we must produce accurate models for each cluster lens.

What has been done?

- Successful source reconstructions. However, **systematic errors in models have become dominant source of error because of improvements in the amount and quality of data. [6]**
- Errors from cluster member selection and image selection have been considered. **[6]**
- **Contribution to lensing by LSS has not been investigated. Is this a dominant source of systematic error?**
- **Check contributions from LSS on models for two HFF fields (Abell 2744, MACS 0416)**

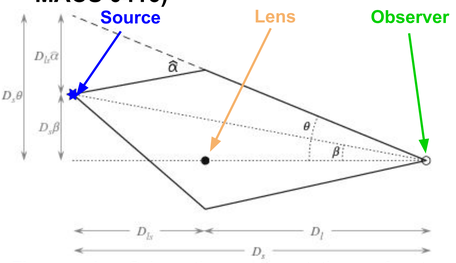

Figure 1: Schematic representation of strong gravitational lensing. This is true if LSS deflection is constant. Figure is adapted from Keeton (2014) **[7]**.

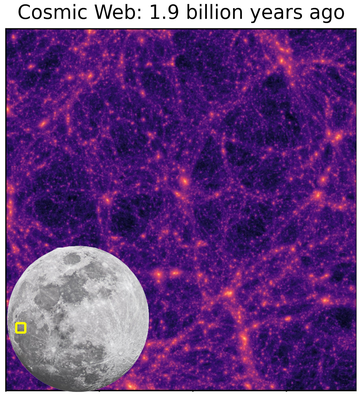

Figure 2: Density plot of simulated LSS (TNG100-3). The full moon has been overlaid for (a rough) scale. The yellow box roughly shows the size of Figure 3.

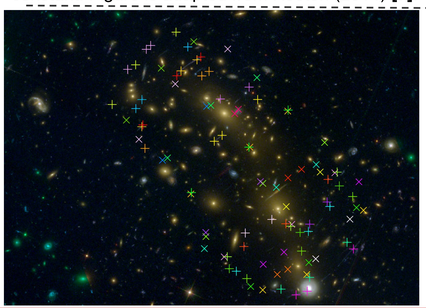

Figure 3: HFF field MACS 0416. The colored symbols indicate gravitationally lensed images. The yellow-orange "blobs" are member and non-member galaxies of the cluster. See Figure 2 for a rough size comparison. Figure modified from Raney et al. **[8].**

Methodology

Step I: Generating Density Maps

- Use **TNG100-3 cosmological simulation [9,10,11,12,13]** to **generate simulated mass density maps of the LSS at various distances** (i.e., redshift) from the observer.
- **Generate 2D histograms of the 3D positions of each particle of each type (gas, dark matter, and stars), weighted by the mass**

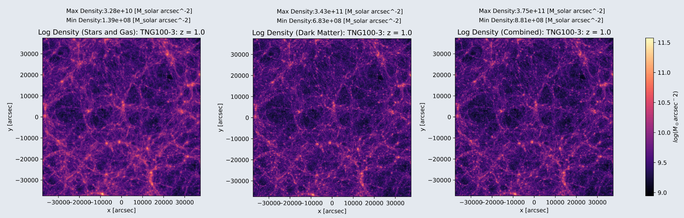

Figure 4: (a) A map of the surface log density for stellar and gas particles in the LSS at redshift 1.0. (b) A map of the surface log density for dark matter particles in the LSS at the same redshift. (c) Map of the surface log density for all three particles combined.

Step II: Computing Deflection Maps

- Define the **surface mass density**, Σ
- Introduce the **lensing potential** ψ (deflection vector is the gradient of the potential). **Solve the Poisson equation (below) using Fourier transforms.**

$$\nabla^2\psi = \frac{\kappa}{\Sigma_{\rm crit}}, \qquad \Sigma_{\rm crit} = \frac{c^2}{4\pi G}\frac{D_S}{D_L D_{LS}}.$$

- Using ψ, find the deflection vector, and hence the deflection map for each snapshot.

Step III: Computing Deflection Statistics

- We arrange the **deflection maps by redshift.** Then, we **use multiplane lens equation and ray-tracing to find total deflection map (TDM).**
- Using TDM, we calculate total deflection of each image in the HFF clusters: Abell 2774 **[14]** and MACS 0416 **[15]**.
- We actually want contributions from high-order terms of deflection.
  - **Fit for zeroth and first order terms of deflection.**
  - **Subtract fit from total deflection**
  - **Subtract "dummy" image deflection.**

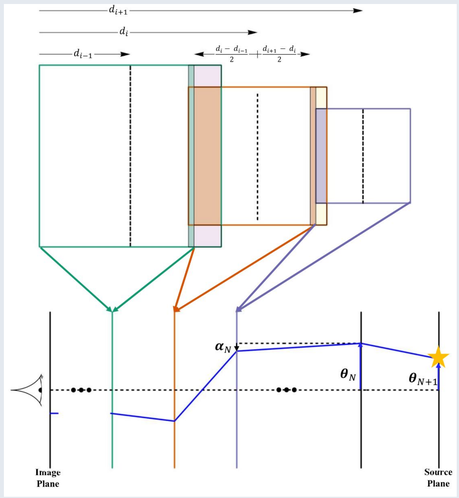

Figure 5: Top: Representation of simulation boxes. Bottom: each box is projected into a plane, and the overall light bending is computed using the multiplane lens equation. Redshift increases to the right.

$$\vec{\delta}_i = \vec{\alpha}_{{\rm sim},i} - \vec{\alpha}_{{\rm fit},i} - \vec{\alpha}_D.$$

$$\alpha_{{\rm fit},(x,i)} = \hat{d}[(\kappa+\gamma_c)x_i + \gamma_s y_i + a_{x,i}]$$
$$\alpha_{{\rm fit},(y,i)} = \hat{d}[\gamma_s x_i + (\kappa-\gamma_c)y_i + a_{y,i}]$$

Results

I. Deflection Statistics

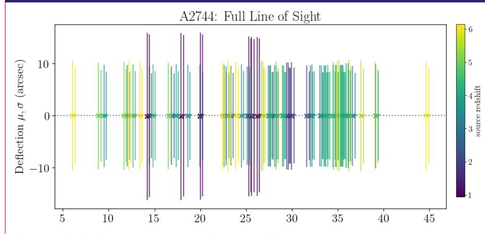

Figure 6: Deflection statistics for Abell 2744 broken up into x and y components for each image.

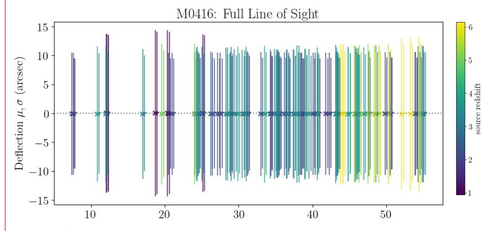

Figure 7: Deflection statistics for MACS 0416 broken up into x and y components for each image.

Cluster	$\overline{\mu}$ (")	$\overline{\sigma}$ (")	RMS (")
A2744	-0.053	9.084	14.100
M0416	-0.055	10.085	15.420

Figure 8: Deflection statistics (average mean deflection, average standard deviation, and RMS deflection) in arcseconds.

- Average mean deflection is approximately zero.
- **Average standard deviation is very high. Indicates LSS deflection varies considerably.**
- **RMS deflections are two orders of magnitude larger than residuals between current models and data.**
  - **Including LSS contributions will substantially change model parameters.**

II. Convergence and Shear Analysis

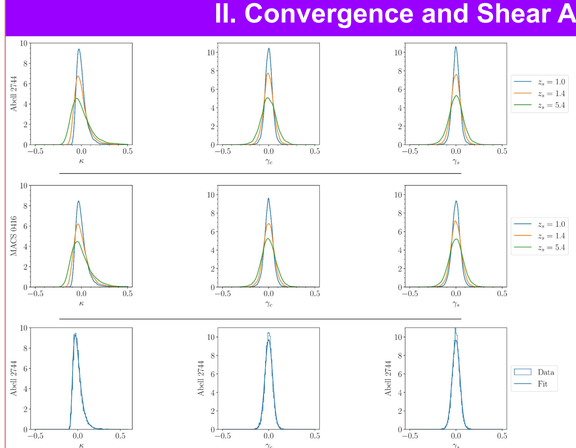

Figure 9: Convergence and shear (κ, γ) distributions for three redshifts (chosen to clearly demonstrate time evolution). These distributions can be used as information (priors) to constrain future lens models.

Future Direction

- **Large standard deviations in deflections suggest attempts to take LSS deflection to be constant is not valid.**
- **We are not justified in neglecting LSS deflection because of the size of the RMS residuals.**
- **We will use results from our analysis with modeling frameworks developed by Raney et al. (2021) to further investigate LSS contribution to cluster lens models.**

Citations

[1] Peacock, J. A., Cole, S., Norberg, P., et al. 2001, , 410, 169
[2] Lotz J. M., et al., 2017, ApJ, 837, 97
[3] Kikuchihara S., et al., 2020, ApJ, 893, 60
[4] Furtak L. J., Atek H., Lehnert M. D., Chevallard J., Charlot S., 2021, MNRAS, 501, 1568
[5] Frye B. L., et al., 2023, ApJ, 952, 81
[6] Raney C. A., Keeton C. R., Brennan S., Fan H., 2020b, MNRAS, 494, 4771
[7] Keeton, C. 2014, Principles of Astrophysics: Using Gravity and Stellar Physics to Explore the Cosmos
[8] Raney, C. A., Keeton, C. R., & Brennan, S. 2020, MNRAS, 492, 503
[9] Naiman J. P., et al., 2018, Monthly Notices of the Royal Astronomical Society, 477, 1206
[10] Nelson D., et al., 2017, Monthly Notices of the Royal Astronomical Society, 475, 624
[11] Marinacci F., et al., 2018, Monthly Notices of the Royal Astronomical Society
[12] Pillepich A., et al., 2017, Monthly Notices of the Royal Astronomical Society, 475, 648
[13] Springel V., et al., 2017, Monthly Notices of the Royal Astronomical Society, 475, 676
[14] Abell G. O., Corwin Harold G. J., Olowin R. P., 1989, ApJS, 70, 1
[15] Ebeling H., Edge A. C., Henry J. P., 2001, ApJ, 553, 66800
[16] Raney, C. A., Keeton, C. R., & Zimmerman, D. T. 2021, MNRAS, 508, 5587

Acknowledgments

I would like to thank Dr. Charles Keeton for his support and mentorship throughout this project. I would also like to thank Dr. Somayeh Khakpash, Dilys Ruan, and Lana Eid for their guidance, and for providing unique and helpful perspectives at various stages. Thirdly, I would like to thank the Aresty Research Center for making this symposium possible. We acknowledge support from the US National Science Foundation for their support through grant AST-1909217.